International Journal of Physical Sciences Vol. 4 (6), pp. 385-389, June, 2009
Available online at http://www.academicjournals.org/IJPS
ISSN 1992 - 1950 © 2009 Academic Journals

Full Length Research Paper

The analytical and numerical investigation of thermo-optic effects in double-end-pumped solid state lasers

F. Kalantarifard[1], H. Nadgaran[2] and P. Elahi[3]

[1]Department of Physics, Payame Noor University, Shiraz, Iran.
[2]Department of Physics, Shiraz University, Shiraz, Iran.
[3]Department of Physics, College of Science, Shiraz University of Technology, Shiraz, Iran.

Accepted 11 June, 2009

In this paper, thermal effects in double-end pumped Nd:YVO$_4$ laser crystal have been investigated. The analytical expression for temperature distribution and thermo-optic effects such as temperature-dependent change of refractive index (dn/dT effect) and end effect have been calculated and the results then applied to Nd:YVO$_4$ crystal., Our analytical model compared with exact numerical calculations and good consistency has been shown.

Key words: Double end pumped, thermo-optic effects, Nd:YVO$_4$ crystal.

INTRODUCTION

Diode pumped solid-state lasers have many advantages with respect to other traditional flash lamped lasers. They have high beam quality and high beam overlap efficiency due to their good pump mode matching with resonator modes (Chen et al., 1999). In middle and high power regime, thermal effects such as thermal lensing and depoarization have most limitation in the laser performance and can not be neglected (Nadgaran et al., 2006, Schmid et al., 2000, Koechner et al., 1970). The heat load due to quantum defects, influence on the beam quality and the laser resonator stability range. There are many ways to reduce thermal effects in the literatures, for example, using composite crystal (MacDonald et al., 2000) and designing the variable configuration resonators (Graf et al., 2001). In this way double-end-pumped (Ogilvy et al., 2003, Ai-Yun et al., 2005) are more noticeable because they extend the stability range of the laser resonator and also thermal loading due to pump source divided between the 2 ends of the laser crystal.

In this work, we consider a double-end-pumped laser configuration. The crystal laser rod is allowed to be pumped from both 2 sides. The heat equation has been solved analytically and an expression for total focal length due to temperature dependent change of refractive index and end effect has been derived. The results then applied to a Nd:YVO$_4$ laser crystal and have compared with numerical calculation results. The figures show good consistency between our theoretical model and exact numeric solution.

THEORETICAL MODELS

Consider a double-end-pumped solid state lasers. The steady state heat equation in an axially symmetric rod is written as

$$\frac{\partial^2 T(r,z)}{\partial r^2}+\frac{1}{r}\frac{\partial T(r,z)}{\partial r}+\frac{\partial T(r,z)}{\partial z}=-\frac{Q_1(r,z)}{k}-\frac{Q_2(r,z)}{k}, \tag{1}$$

where k is thermal conductivity, $Q_1(r,z)$ and $Q_2(r,z)$ are the heat power density due to left and right pump respectively. For high power end-pumped lasers, $Q(r,z)$ can be described as a top-hat distribution as

$$Q_1(r,z)=\frac{1}{\pi a^2}\left[\frac{\zeta P_1\alpha_1}{1-\exp(-\alpha_1 L)}\right]e^{-\alpha_1 z}\Theta(r-a), \tag{2}$$

$$Q_2(r,z)=\frac{1}{\pi a^2}\left[\frac{\zeta P_2\alpha_2}{\exp(\alpha_2 L)-1}\right]e^{\alpha_2 z}\Theta(r-a). \tag{3}$$

In the above equations z is the distance from the left side of the crystal, ζ is heat load fraction, a is the pump radius, L is the crystal length, $P_1(P_2)$ are the left (right)

*Corresponding author. E-mail: elahi@sutech.ac.ir

absorbed pump power and $\alpha_1(\alpha_2)$ are the absorption coefficient of the crystal at the pump wavelength at input power $P_1(P_2)$, and $\Theta(r-a)$ is defined as

$$\Theta(r-a)=\begin{cases}1 & r\le a\\ 0 & r>a.\end{cases} \qquad (4)$$

The absorption coefficient is related to the pump power and can be described as

$$\alpha_{1(2)}=\frac{\alpha_0}{1+\dfrac{P_{1(2)}}{P_{sat}}}, \qquad (5)$$

Where α_0 is the small signal absorption coefficient and P_{sat} is the saturation pump power. We consider the surface cooled configuration and the case which the crystal is greater than the radius the *z* derivative in heat equation can be neglected. Using the following boundary conditions including the continuity of temperature and gradient on the boundary of the pump region means

$$T_{pump}(r=a)=T_{unpum}(r=a), \qquad (6)$$

And

$$\frac{\partial T_{pump}(r=a)}{\partial T}=\frac{\partial T_{unpump}(r=a)}{\partial T}, \qquad (7)$$

and the Newtonian boundary condition of cooling as

$$\left.\frac{\partial T_{unpump}(r)}{\partial r}\right|_{r=a}=\frac{h}{k}\left[T_c-\left.T_{unpump}(r)\right|_{r=a}\right], \qquad (8)$$

We find the following relations for temperature distribution within and out of pump regions as

$$T_{pump}(r,z)=T_0-\frac{1}{4\pi a^2k}\left[\left[\frac{\zeta P_1\alpha_1}{1-\exp(-\alpha_1L)}\right]e^{-\alpha_1z}+\left[\frac{\zeta P_2\alpha_2}{\exp(\alpha_2L)-1}\right]e^{\alpha_2z}\right]r^2 \quad r\le a \qquad (9)$$

And

$$T_{unpump}(r,z)=T_0-\frac{1}{4\pi k}\left[\left[\frac{\zeta P_1\alpha_1}{1-\exp(-\alpha_1L)}\right]e^{-\alpha_1z}+\left[\frac{\zeta P_2\alpha_2}{\exp(\alpha_2L)-1}\right]e^{\alpha_2z}\right](1+\ln(\frac{r}{a})) \quad r\ge a \qquad (10)$$

The temperature distribution can be rewritten as follow

$$T(r,z)=T_0-\frac{1}{\pi a^2k}\left[\left[\frac{\zeta P_1\alpha_1}{1-\exp(-\alpha_1L)}\right]e^{-\alpha_1z}+\left[\frac{\zeta P_2\alpha_2}{\exp(\alpha_2L)-1}\right]e^{\alpha_2z}\right]\left[\Theta(r-a)(\frac{r^2}{a^2}-1-\ln(\frac{r}{a}))+(1+\ln(\frac{r}{a})\right], \qquad (11)$$

Where T_0 is the temperature at $z=0$ and given by

$$T_0=Tc+\left[\frac{\frac{1}{\pi}\left[\frac{\zeta P_1\alpha_1}{1-\exp(-\alpha_1L)}\right]e^{-\alpha_1z}+\frac{1}{\pi}\left[\frac{\zeta P_2\alpha_2}{\exp(\alpha_2L)-1}\right]e^{\alpha_2z}}{4k}\right]\left[2Ln\left(\frac{b}{a}\right)-\frac{2k}{bh}+1\right]. \qquad (12)$$

Where T_C is the coolant temperature. The inhomogeneous temperature distribution in the laser materials, generate some thermo-optic effects called dn/dT and end effects.

Dn/DT EFFECT

Consider a cylindrical rod in which r is its radial coordinate and z is measured along the length of cylinder. The refractive index, n, of rod is usually a function of r, z, and T, where T is the temperature. Expanding the refractive index about temperature of the center of the rod, T_0, we have

$$n(r,z,T)=n(r,z,T_0)+(T-T_0)\frac{dn}{dT}+\frac{1}{2}(T-T_0)^2\frac{d^2n}{dT^2}+....., \qquad (13)$$

where $\frac{dn}{dT}$, $\frac{d^2n}{dT^2}$ are thermo-optic coefficient of the crystal and are constant values depends on the crystal properties. By neglecting the higher order terms, we have (Koechner, 1999)

$$n(r,z,T)-n(r,z,T_0)=\Delta n(r,z)_T=\left[T(r,z)-T_0\right]\frac{dn}{dT}, \qquad (14)$$

This effect called dn/dt effects or temperature dependent change of refractive index effect. By substituting Eq. (9) into Eq. (14), the dn/dT effect in the pumped region will be

$$\Delta n(r,z)_T=-\frac{\frac{dn}{dT}}{\pi a^2k}\left[\left[\frac{\zeta P_1\alpha_1}{1-\exp(-\alpha_1L)}\right]e^{-\alpha_1z}+\left[\frac{\zeta P_2\alpha_2}{\exp(\alpha_2L)-1}\right]e^{\alpha_2z}\right]r^2. \qquad (15)$$

The overall phase shift then can be obtained by (Koechner, 1999)

$$\Delta\phi(r)_T = \frac{2\pi}{\lambda}\int_0^L \Delta n(r,z)_T\, dz. \tag{16}$$

By using the equation (15) and (16), the overall phase shift can be calculated as

$$\Delta\phi(r)_T = \frac{\zeta \frac{dn}{dT}}{2a^2 k}\left[P_1 + P_2\right] r^2. \tag{17}$$

Finally the induced focal length due to dn/dT effect, $f_{\frac{dn}{dT}}$, can be obtained from

$$f_{\frac{dn}{dT}} = -\frac{\pi}{\Delta\phi(r)_T} r^2 = \frac{2\pi a^2 k}{\zeta \frac{dn}{dT}\left[P_1 + P_2\right]}. \tag{18}$$

As see from the above equation the focal length due to dn/dT effect is dependent on the total pumped power.

END-EFFECT

Elongation of the laser rod due to temperature can be obtained as (Koechner, 1999)

$$l(r) = \alpha_T \int_0^{l_0} \Delta T(r,z)_T\, dz, \tag{19}$$

Where l_0 is the ordinary length of the rod over which the elongation takes place and is usually assumed to be approximately equal to the radius of crystal, and $\Delta T(r,z)$ is the temperature difference. By inserting the temperature difference according to Eq. (9), after simplifying, the left side elongation can be obtained as:

$$\text{l1} = \frac{\alpha_T \zeta}{4\pi k a^2}\left[\frac{P_1\left(\exp(-\alpha_1 a) - 1\right)}{1 - \exp(-\alpha_1 L)} - \frac{P_2\left(\exp(\alpha_2 a) - 1\right)}{\exp(\alpha_2 L) - 1}\right] r^2. \tag{20}$$

The right side elongation can also be obtained as

$$\text{l1} = \frac{\alpha_T \zeta}{4\pi k a^2}\left[\frac{P_1 \exp(-\alpha_1 L)\left(1 - \exp(\alpha_1 a)\right)}{1 - \exp(-\alpha_1 L)} - \frac{P_2\left(\exp(\alpha_2 a) - 1\right)}{\exp(\alpha_2 L) - 1}\right] r^2. \tag{21}$$

The radius of curvature then according to

$$R_{1,2} = \left(\frac{d^2 l_{1,2}}{d r^2}\right)^{-1}, \tag{22}$$

will be

$$R_1 = \left\{\frac{-\alpha_T \zeta}{2\pi k a^2}\left[\frac{P_1\left(\exp(-\alpha_1 a) - 1\right)}{1 - \exp(-\alpha_1 L)} - \frac{P_2\left(\exp(-\alpha_2 a) - 1\right)}{\exp(\alpha_2 L) - 1}\right]\right\}^{-1}, \tag{23}$$

and

$$R_2 = \left\{\frac{-\alpha_T \zeta}{2\pi k a^2}\left[\frac{P_1 \exp(-\alpha_1 L)\left(1 - \exp(\alpha_1 a)\right)}{1 - \exp(-\alpha_1 L)} - \frac{P_2\left(1 - \exp(-\alpha_2 a)\right)}{1 - \exp(-\alpha_2 L)}\right]\right\}^{-1}, \tag{24}$$

Where R_1 and R_2 are radius of curvature of the left and right surfaces of the crystal respectively. By using the radius of curvature the left and right focal length due to end effect will be

$$f_{1,2End} = \frac{R_{1,2}}{2(n-1)}. \tag{25}$$

So the total focal length can be written as

$$\frac{1}{f_{tot}} = \frac{1}{f_{1End}} + \frac{1}{f_{2End}} + \frac{1}{f_{\frac{dn}{dT}}}. \tag{26}$$

RESULTS AND DISCUSSION

In this part, the analytical formula derived in the previous parts will apply for a typical Nd:YVO_4 laser crystal and compare with exact numerical calculations to obtain much accurate results. We consider a double end pump laser crystal with radius 5 mm and length of 12 mm. Figures 1a and b, shows the temperature distribution in one half an axial cross section for a left pump power as P_1=10W , right pump power as P_2 = 5W and a = 0.2 cm. As see from these figures, the maximum temperature raise to 385 K.

Now we consider the total pump power as a constant value. For this reason we consider P_1 + P_2 =15 W. By substituting P_2 = 15-P1 in the obtained relations, the temperature distribution on the axis of crystal versus input left power and z has been plotted in Figures 2. In Figure 2a and 2b the pump radius is 0.2 mm and 0.1 mm respectively. We see that the maximum temperature will

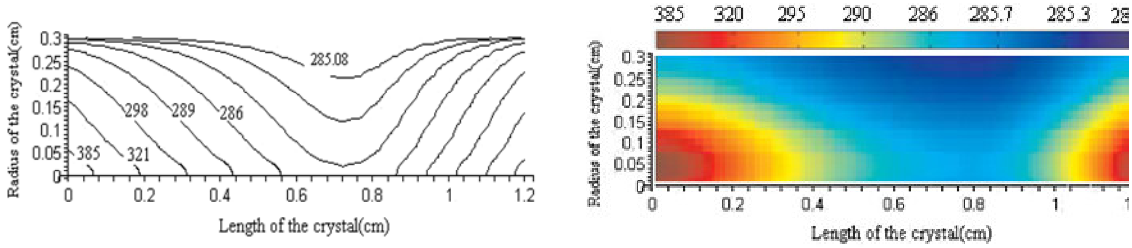

(a) (b)

Figure 1. (a) The temperature distribution in the Nd:YVO_4 laser crystal. (1b) Heat diagram in the Nd:YVO_4 laser crystal pumped by10 and 5 Watts from left and right side respectively. Pumped by 10 and 5 Watts from left and right side.

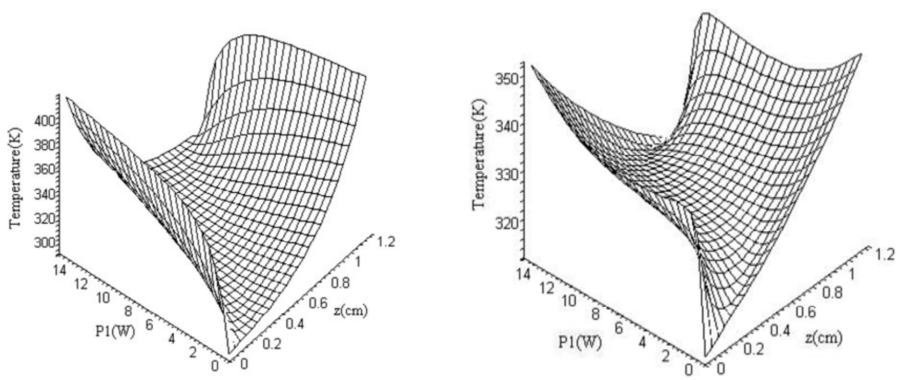

(a) (b)

Figure 2. Temperature on the axis of Nd:YVO_4 crystal versus left pump power and distance from left surface for a = 0.2 mm. (b) Temperature on the axis of Nd:YVO_4 crystal versus left pump power and distance from left surface for a = 0.1 mm.

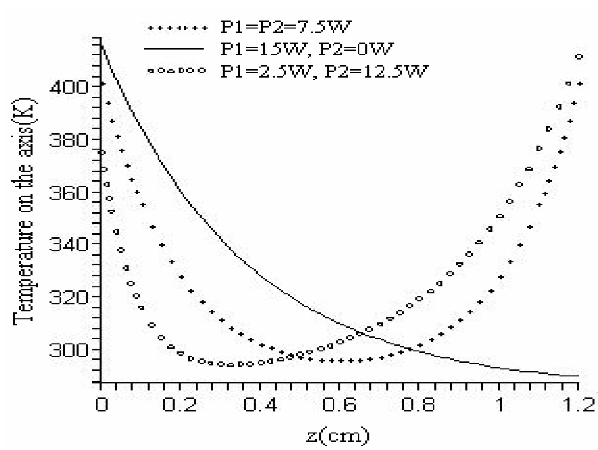

Figure 3. Temperature distribution versus z for three kind of pumping

decrease with decreasing pump radius. It is important to note that by decreasing the pump radius, a relative maximum will appear in the figure near 2 side of the crystal which is due to increasing heat power density.

As see from Figure 3, the maximum temperature will be decreased in double configuration and is minimum for equal pumping. The total focal length due to temperature dependent change of refractive index and end effect versus left input pump power for a = 0.2 mm, a = 0.15 mm and a = 0.1 mm have been plotted in Figures 4a, 4b and 4c respectively. As see from these figures, the total focal length decrease by decreasing pump radius. In Figures 4a and 4b, the maximum and minimum total focal length appear in single and double end pumped with equal pumping respectively. Although the double-end-pumped configuration extend the stability of resonator, but will increase the thermal induced focal length. Another important result is appearing a relative maximum by decreasing pump radius in the total focal length curves. So, for small pump radius the best configuration is pumping with equal power. The numerical calculation has been compared with our analytical solution in these figures. We can see that the difference between analytical and numerical result is quite small.

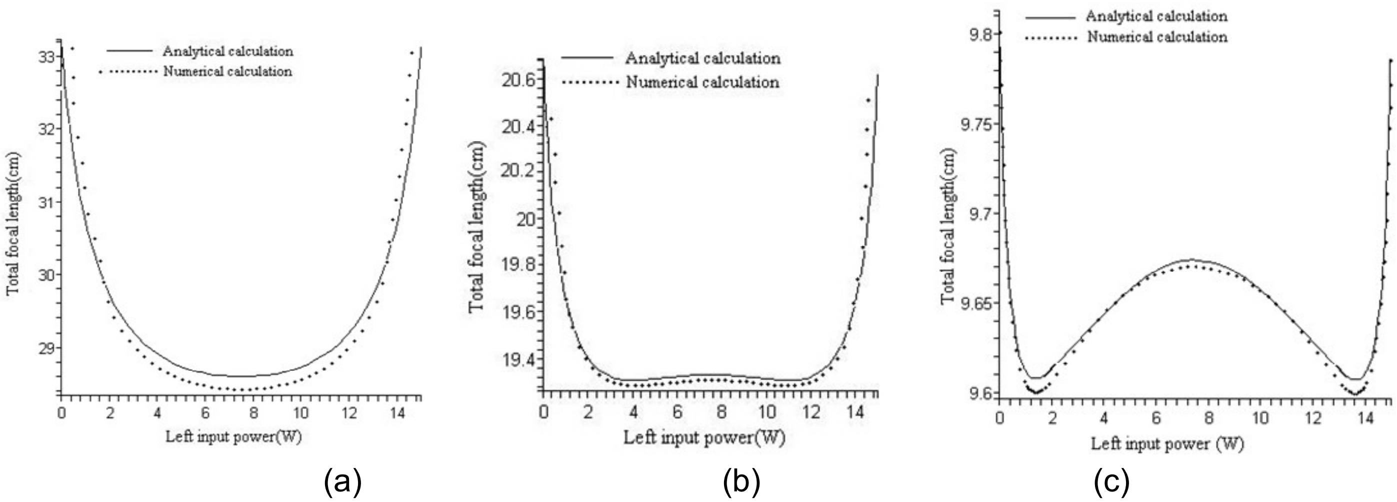

Figure 4. (a) Total focal length versus left versus left input power for 0.2 mm pump radius. (b) Total focal length versus left input power for 0.150 mm pump radius. (c) Total focal length input power for 0. 1 mm pump radius.

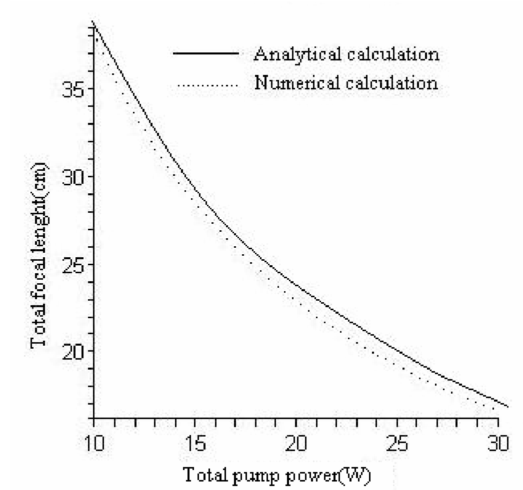

Figure 5. Comparison between analytical model (solid line) and numeric (doted line)

In Figure 5 we plotted the total focal length in equal end pumping configuration versus total pump power. We see the good consistency between analytical and numerical calculation ion this figure.

Conclusion

In this paper the heat distribution and then heat induced total focal length have been investigated by analytical model in double-end-pumped solid state laser and compared with numerical calculation. Double pumped configurations are useful for high power regime because of wide stability resonator range. While single end-pumping approach the crystal fracture limit, double-end-pumped configuration reduce risk of future by dividing thermal load between the two end surfaces. But it is important notice that single-pumped configuration produce greater total focal length and the thermo-optic effects will be less. By using the proper pump radius such for example for a = 0.1 mm, the relative maximum in the total focal length versus input power shows that the best configuration for reducing thermo-optic effects is equal double pumped.

REFRENCES

Chen YF, Huang TM, Liao CC, Lan YP, Wang SC (1999). Efficient high-power diode-end-pumped TEM_{00} $Nd:YVO_4$ lasers, IEEE Photonics Technol. Lett. 11: 1241.

Graf TH, Wyss E, Roth M, Weber HP (2001). Laser resonator with balanced thermal lenses, Opt. Commun. 190: 327-331.

Koechner W, Rice DK (1970). Effect of birefringence of line-early polarized YAG:Nd lasers , IEEE J.Quantum Electron., 6(9): 557-566

Koechner W (1999). Solid State Laser Engineering, pp. 408. 5th ed., Springer.

MacDonald MP, Graf TH, Balmer JE, Weber HP (2000). Reducing thermal lensing in diode-pumped laser rods, Opt. Commun., 78: 383-393.

Nadgaran H, Elahi P (2006). Numerical simulation and analytical description of thermally induced depolarization in diode-pumped laser rods pumped by a super-Gaussian beam, Int. J. Pure and Applied Physics, 2(3): 215-221.

Nadgaran H, Elahi P (2006), The overall phase shift and lens effect calculation using Gaussian boundary conditions and paraxial ray approximation for an end-pumped solid-state laser, *Pramana*- J. Phys. 66(3): 513-519.

Ogilvy H, Withford M, Dekker J, James P, Piper A (2003). Efficient diode double-end-pumped $Nd:YVO_4$ Lser operating at 1342 nm, Opt. Express 11(19): 2411-2414.

Schmid M, Weber R, Graf TH, Rooz M, Weber HP (2000). Numerical simulation and analytical description of thermally induced birefringence in laser rods , IEEE J. Quantum Electron, 36: 620-626.

Ai-Yun Y (2005). Double-end-pumped 11-W $Nd:YVO_4$ cw laser at 1342 nm, J. Opt. Soc. Am. B,22 (10): 2129-2133.